JACS
JOURNAL OF THE AMERICAN CHEMICAL SOCIETY

Article

pubs.acs.org/JACS

Targeted Theranostic Platinum(IV) Prodrug with a Built-In Aggregation-Induced Emission Light-Up Apoptosis Sensor for Noninvasive Early Evaluation of Its Therapeutic Responses in Situ

Youyong Yuan,[†] Ryan T. K. Kwok,[‡] Ben Zhong Tang,*[,‡,§] and Bin Liu*[,†,∥]

[†]Department of Chemical and Biomolecular Engineering, National University of Singapore, 4 Engineering Drive 4, Singapore 117585

[‡]Department of Chemistry, Institute of Molecular Functional Materials, Division of Biomedical Engineering, The Hong Kong University of Science and Technology, Clear Water Bay, Kowloon, Hong Kong

[§]SCUT-HKUST Joint Research Laboratory, Guangdong Innovative Research Team, State Key Laboratory of Luminescent Materials and Devices, South China University of Technology, Guangzhou China 510640

[∥]Institute of Materials Research and Engineering, 3 Research Link, Singapore 117602

Supporting Information

ABSTRACT: Targeted drug delivery to tumor cells with minimized side effects and real-time in situ monitoring of drug efficacy is highly desirable for personalized medicine. In this work, we report the synthesis and biological evaluation of a chemotherapeutic Pt(IV) prodrug whose two axial positions are functionalized with a cyclic arginine−glycine−aspartic acid (cRGD) tripeptide for targeting integrin $\alpha_v\beta_3$ overexpressed cancer cells and an apoptosis sensor which is composed of tetraphenylsilole (TPS) fluorophore with aggregation-induced emission (AIE) characteristics and a caspase-3 enzyme specific Asp-Glu-Val-Asp (DEVD) peptide. The targeted Pt(IV) prodrug can selectively bind to $\alpha_v\beta_3$ integrin overexpressed cancer cells to facilitate cellular uptake. In addition, the Pt(IV) prodrug can be reduced to active Pt(II) drug in cells and release the apoptosis sensor TPS-DEVD simultaneously. The reduced Pt(II) drug can induce the cell apoptosis and activate caspase-3 enzyme to cleave the DEVD peptide sequence. Due to free rotation of the phenylene rings, TPS-DEVD is nonemissive in aqueous media. The specific cleavage of DEVD by caspase-3 generates the hydrophobic TPS residue, which tends to aggregate, resulting in restriction of intramolecular rotations of the phenyl rings and ultimately leading to fluorescence enhancement. Such noninvasive and real-time imaging of drug-induced apoptosis in situ can be used as an indicator for early evaluation of the therapeutic responses of a specific anticancer drug.

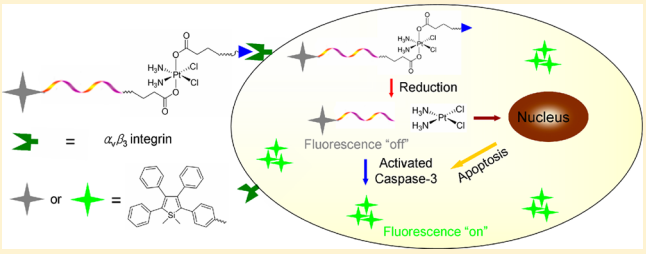

INTRODUCTION

Drug delivery systems have been widely used for improving cancer therapeutic efficiencies of small-molecule drugs.[1] Typically, the anticancer drugs are loaded or covalently conjugated to the delivery systems and are expected to release only at specific tumor sites. Development of strategies for real-time monitoring of drug delivery/release at target cancer cells is a very important step to indirectly evaluate the potential therapeutic efficiency.[2] The most common strategy is to use fluorescent dyes/drugs as model cargo systems. However, such strategy faces some problems, e.g. difficulties in correlating the release of the fluorescent dyes to the actual drug molecules, or the restricted usage of limited fluorescent drugs (e.g., doxorubicin). Recently, some theranostic prodrug delivery systems have been developed for real-time monitoring of the release of active drugs by conjugating the drugs with fluorescent dyes.[3] The design strategy relies on drug release-induced fluorescence intensity or color change upon tumor-associated stimulus. Most of the systems reported so far are focused on monitoring the delivery and/or release of the drugs. However, no direct information is given for the therapeutic effect, which requires further experiments to evaluate. The early evaluation of cancer's response to a specific therapy is of high importance in clinical applications because it can minimize the duration of ineffective courses in cancer therapy. Currently, the common method to evaluate the effectiveness of cancer treatment is by measuring the tumor size using magnetic resonance imaging (MRI).[4] However, MRI technique is unsatisfactory in evaluating the early response of cancer to a particular therapeutic drug as the change in tumor size is not obvious at the early stages of therapy. As a consequence, it is highly desirable if one could design and develop a theranostic system that can simultaneously deliver the therapeutic drugs and noninvasively evaluate the therapeutic responses in situ.

One of the most promising solutions to this issue is to incorporate an apoptosis sensor into the system. As therapeutic drugs generally kill the cancer cells by activating apoptosis

Received: November 20, 2013
Published: January 17, 2014

   dx.doi.org/10.1021/ja411811w | J. Am. Chem. Soc. 2014, 136, 2546−2554

Scheme 1. Schematic Illustration of the Targeted Theranostic Platinum(IV) Prodrug with a Built-In Aggregation-Induced Emission (AIE) Light-Up Apoptosis Sensor for Noninvasive in Situ Early Evaluation of Its Therapeutic Responses

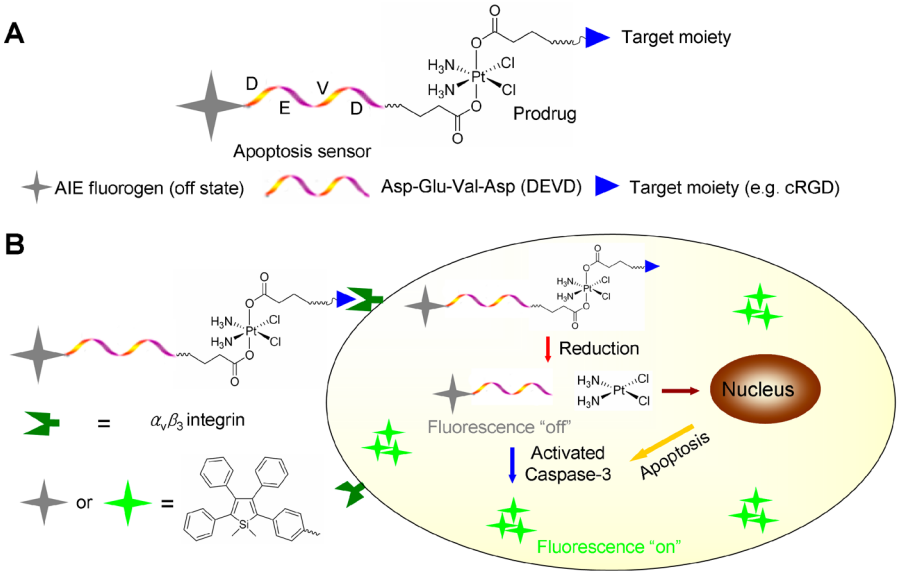

within a short period of time, the apoptosis sensor could evaluate the therapy efficacy at a very early stage.[5] So far, several strategies have been utilized for detection of cell apoptosis on the basis of the alterations of apoptosis-associated biochemical substances within the cells.[6] One of the most important pathways of therapeutic drug-induced apoptosis is activation of caspase-3, a cysteine protease which specifically cleaves proteins containing the Asp-Glu-Val-Asp (DEVD) peptide sequence.[7] Recently, we have developed a simple strategy for real-time monitoring of cell apoptosis in vitro and in vivo based on probes containing fluorogens with aggregation-induced emission (AIE) characteristics.[8] These probes are nonemissive in molecularly dissolved stated, but the caspase-3 cleaved AIE residues are highly emissive due to the restriction of intramolecular rotations (RIR), which reduces energy dissipation via nonradiative channels.[9] Although these probes are able to respond to drug-induced apoptosis, they are not able to report the exact drug location or quantify the therapeutic responses in situ as the probes and drugs may not be in the same cells or the probe is not colocalized with the drug when they are in the same cells. It is highly desirable to develop a theranostic drug delivery system that could also evaluate the therapeutic response in situ.

Platinum drug is one of the most effective therapeutic agents against many cancers.[10] In clinics, cisplatin (*cis*-dichlorodiammineplatinum(II)) is one of the most widely used anticancer drugs which can bind to DNA and induce cell apoptosis.[11] However, like most of the other small-molecule anticancer drugs, its clinical use is limited due to the severe side effects.[10b] A promising strategy to minimize the side effect of platinum drug is to employ targetable nontoxic Pt(IV) complexes as prodrugs which can be intracellularly activated by reduction to the toxic Pt(II) form.[12] Receptor-targeted chemotherapeutics are attractive because they target receptors that are overexpressed in tumors so that they can minimize systematic distribution of the drugs and facilitate their binding and internalization in cells that express the specific receptor.[1a] The greater inertness of Pt(IV) complexes makes the prodrug more stable in blood and thus has the potential to accumulate in the tumor site. The prodrug can also avoid undesirable interactions with proteins and other biomolecules in blood circulation to reduce the side effects. As a consequence, targeted delivery of a Pt(IV) prodrug with a built-in apoptosis sensor would be an ideal strategy for simultaneous drug delivery with reduced side effects and noninvasive early evaluation of its therapeutic responses in situ.

In this contribution, we developed a targetable theranostic Pt(IV) prodrug with a special focus on monitoring drug-induced cell apoptosis in situ. The system is composed of a chemotherapeutic Pt(IV) prodrug which can be reduced to active Pt(II) intracellularly, an apoptosis sensor (TPS-DEVD) based on tetraphenylsilole (TPS) with AIE characteristics, and a cyclic(RGD) peptide as the targeting ligand (Scheme 1). The prodrug can accumulate preferentially in cancer cells with overexpressed $\alpha_v\beta_3$ integrin and release the active drug Pt(II) and apoptosis sensor TPS-DEVD upon the intracellular reduction of the Pt(IV) prodrug. The released Pt(II) can induce cell apoptosis and activate caspase-3 to cleave the DEVD peptide in TPS-DEVD and trigger the fluorescence. The fluorescence turn-on response allows us to utilize the theranostic platform for real-time and noninvasive imaging of the therapeutic responses of a specific anticancer drug.

EXPERIMENTAL SECTION

General Information. Cisplatin, *N*,*N*-diisopropylethylamine (DIEA), *N*-hydroxysuccinimide (NHS), 1-ethyl-3-[3-dimethylaminopropyl]carbodiimide hydrochloride (EDC), copper(II) sulfate ($CuSO_4$), sodium ascorbate, ascorbic acid, succinic anhydride, 3-(4,5-dimethylthiazol-2-yl)-2,5-diphenyltetrazolium bromide (MTT), anhydrous dimethyl sulfoxide (DMSO), anhydrous dimethylformamide (DMF), lithium wires, naphthalene, 4-bromobenzene, 4-bromobenzyl bromide, sodium azide, dichlorobis(triphenylphosphine)palladium(II), $ZnCl_2$·TMEDA, piperazine-*N*,*N*′-bis(2-ethanesulfonic acid) (PIPES), diethyldithiocarbamate (DDTC), bovine serum albumin (BSA), lysozyme, pepsin, trypsin and other chemicals were all purchased from Sigma-Aldrich and used as received without further purification. Hexane and tetrahydrofuran

dx.doi.org/10.1021/ja411811w | J. Am. Chem. Soc. 2014, 136, 2546−2554

(THF) purchased from Fisher Scientific were distilled from sodium benzophenoneketyl immediately prior to use. Dichloromethane (DCM) was distilled over calcium hydride. Deuterated solvents with tetramethylsilane (TMS) as internal reference were purchased from Cambridge Isotope Laboratories Inc. Alkyne-functionalized DEVD (Asp-Glu-Val-Asp-Pra) and amine-functionalized cRGD (cyclic(Arg-Gly-Asp-D-Phe-Lys)) were customized from GL Biochem Ltd. *cis,cis,trans*-Diamminedichlorodisuccinatoplatinum(IV) was synthesized following a literature method.[13]

Dulbecco's Modified Essential Medium (DMEM) is a commercial product of National University Medical Institutes (Singapore). Milli-Q water was supplied by Milli-Q Plus System (Millipore Corporation, Breford, United States). Piperazine-*N*,*N*′-bis(2-ethanesulfonic acid) (PIPES) buffer containing 50 mM PIPES, 100 mM NaCl, 1 mM ethylenediaminetetraacetic acid (EDTA), 0.1% w/v 3-[(3-cholamidopropyl)-dimethylammonio] propanesulfonic and 25% w/v sucrose (pH = 7.2). Recombinant human caspase-3 was purchased from R&D Systems. Caspase-3 inhibitor 5-[(*S*)-(+)-2-(methoxymethyl)pyrrolidino]sulfonylisatin was purchased from Calbiochem. Fetal bovine serum (FBS) and trypsin−EDTA solution were purchased from Gibco (Lige Technologies, AG, Switzerland). Staurosporine (STS) was purchased from Biovision. DRAQ5 was purchased from Biostatus. Cleaved caspase-3 (Asp175) (5A1E) rabbit mAb (#9664) was purchased from Cell Signaling. Mouse anti-rabbit IgG-TR (sc-3917) was purchased from Santa Cruz.

Characterization. NMR spectra were measured on a Bruker ARX 400 NMR spectrometer. Chemical shifts were reported in parts per million (ppm) referenced with respect to residual solvent ($CDCl_3$ = 7.26 ppm, $(CD_3)_2SO$ = 2.50 ppm or tetramethylsilane $Si(CH_3)_4$ = 0 ppm). Particle size and size distribution were determined by laser light scattering (LLS) with a particle size analyzer (90 Plus, Brookhaven Instruments Co., United States) at a fixed angle of 90° at room temperature. HPLC profiles and mass spectra were acquired using a Shimadzu IT-TOF. A 0.1% TFA/H_2O and 0.1% TFA/acetonitrile were used as eluents for the HPLC experiments. High-resolution mass spectra (HRMS) were recorded on a Finnigan MAT TSQ 7000 mass spectrometer. UV−vis absorption spectra were taken on a Milton Ray Spectronic 3000 array spectrophotometer. Photoluminescence (PL) spectra were measured on a Perkin-Elmer LS 55 spectrofluorometer.

Synthesis of 4-Bromobenzyl Azide. Into a flask equipped with a magnetic stirrer were added 4-bromobenzyl bromide (7.5 g, 30 mmol), sodium azide (7.8 g, 120 mmol), and 40 mL of DMSO. After stirring at 70 °C for 12 h, the solution was poured into 150 mL of water and extracted with DCM. The crude product was purified by silica-gel chromatography using hexane as eluent to give a colorless, viscous liquid in 96% yield (6.12 g). ^{1}H NMR ($CDCl_3$, 400 MHz), δ (TMS, ppm): 7.47 (d, 2H, −CH−), 7.15 (d, 2H, −CH−), 4.26 (s, 2H, $-CH_2-$). ^{13}C NMR ($CDCl_3$, 100 MHz), δ (TMS, ppm): 134.3, 131.8, 129.6, 122.1, 53.9. HRMS (MALDI-TOF): m/z 210.964 (M^+, calcd 210.974).

Synthesis of 1,1-Dimethyl-2-[4-(azidomethyl)phenyl]-3,4,5-triphenylsilole (TPS-CH_2N_3). Dimethylbis-(phenylethynyl)silane was prepared according to our published procedures.[14] A mixture of lithium (0.056 g, 8 mmol) and naphthalene (1.04 g, 8 mmol) in 8 mL of THF was stirred at room temperature under nitrogen for 3 h to form a deep, dark-green solution of LiNaph. A solution of dimethylbis-(phenylethynyl)silane (0.52 g, 2 mmol) in 5 mL of THF was then added dropwise to LiNaph solution at room temperature. After stirring for 1 h, the mixture was cooled to 0 °C and then diluted with 25 mL of THF. A black suspension was formed upon addition of $ZnCl_2$·TMEDA (2 g, 8 mmol). After stirring for an additional hour at room temperature, a solution containing 4-bromobenzene (0.34 g, 2.2 mmol), 4-bromobenzyl azide (0.47 g, 2.2 mmol) and $PdCl_2(PPh_3)_2$ (0.08 g, 0.1 mmol) in 25 mL of THF was added. The mixture was refluxed overnight. After cooling down to room temperature, 100 mL of 1 M HCl solution was added and the mixture was extracted with DCM several times. The organic layer was combined and washed with brine and water and then dried over magnesium sulfate. After solvent evaporation under reduced pressure, the residue was purified by a silica-gel column using hexane as eluent. The product was obtained as a yellow solid in 36% yield (0.34 g). ^{1}H NMR ($CDCl_3$, 400 MHz), δ (TMS, ppm): 7.15−7.06 (m, 6H, −CH−), 7.02−6.99 (m, 5H, −CH−), 6.95−6.93 (m, 4H, −CH−), 6.82−6.79 (m, 4H, −CH−), 4.23 (s, 2H, $-CH_2-$), 0.48 (s, 6H, $-CH_3$). ^{13}C NMR ($CDCl_3$, 100 MHz), δ (TMS, ppm): 154.5, 153.9, 142.1, 141.2, 140.1, 139.8, 138.7, 132.5, 130.0, 129.2, 128.9, 128.0, 127.5, 126.4, 126.3, 125.7, 54.7, −3.80. HRMS (MALDI-TOF): m/z 469.1959 (M^+, calcd 469.1974).

Synthesis of *N*-Hydroxysuccinimide-Activated Platinum(IV) Complexes. A mixture of platinum(IV) complex *cis*, *cis*, *trans*-diamminedichlorodisuccinatoplatinum-(IV) (32.1 mg, 0.06 mmol), EDC (23.0 mg, 0.12 mmol) and NHS (13.8 mg, 0.12 mmol) in anhydrous DMF (1 mL) was stirred at room temperature overnight. After that, the mixture was purified by HPLC (solvent A: water with 0.1% TFA, solvent B: CH_3CN with 0.1% TFA) and quickly lyophilized to yield the desired product as a white powder in 78% yield (34.1 mg). ^{1}H NMR (400 MHz, DMF-d_7), δ (TMS, ppm): 6.92−6.68 (m, 6H, $-NH_3$), 2.94−2.91 (m, 8H, $-CH_2-$), 2.89−2.84 (m, 4H, $-CH_2-$), 2.72−2.68 (m, 4H, $-CH_2-$). ^{13}C NMR (DMF-d_7, 100 MHz), δ (TMS, ppm): 178.5, 170.6, 168.8, 30.0, 27.1, 25.9. IT-TOF-MS: m/z $[M + H]^+$ calcd 728.026, found 728.021.

"Click" Synthesis of Amine-Terminated TPS-DEVD. Alkyne-functionalized DEVD (10.2 mg, 20 μmol) and TPS-CH_2N_3 (9.4 mg, 20 μmol) were dissolved in a mixture of DMSO/H_2O solution (v/v = 1/1; 1.0 mL). The "click" reaction was initiated by sequential addition of catalytic amounts of $CuSO_4$ (9.6 mg, 6 μmol) and sodium ascorbate (2.4 mg, 12 μmol). The reaction was continued with shaking at room temperature for another 24 h. The final product was purified by HPLC and lyophilized under vacuum to yield the probe as white powders in 45% yield (9.4 mg). ^{1}H NMR (DMSO−d_6, 400 MHz): 12.24 (s, 3H, −COOH), 8.49 (d, 1H, −NH−), 8.32 (d, 1H, −NH−), 8.05 (d, 1H, −NH−), 7.92 (d, 1H, −NH−), 7.86 (s, 1H, −CH−), 7.22−7.06 (m, 6H, −CH−), 7.02−6.99 (m, 5H, −CH−), 6.95−6.88 (m, 4H, −CH−), 6.82−6.79 (m, 4H, −CH−), 5.45 (s, 2H, $-CH_2-$), 4.54−4.49 (m, 1H, −CH−), 4.38 (m, 2H, −CH−), 4.17−4.13 (m, 2H, −CH−), 3.10−3.05 (m, 1H, $-CH_2-$), 2.92−2.88 (m, 1H, $-CH_2-$), 2.71−2.65 (m, 2H, $-CH_2-$), 2.26−2.21 (m, 2H, $-CH_2-$), 2.01−1.85 (m, 2H, $-CH_2-$), 0.84−0.74 (m, 6H, $-CH_3$), 0.43 (s, 6H, $-CH_3$); IT-TOF-MS: m/z $[M + H]^+$ calcd 1040.426, found 1040.866.

Synthesis of Theranostic Prodrug TPS-DEVD-Pt-cRGD. Amine-terminated TPS-DEVD (9.0 mg, 8.7 μmol) and amine-

functionalized cRGD (5.2 mg, 8.7 μmol) were dissolved in anhydrous DMSO (1.0 mL) with a catalytic amount of DIEA (1.0 μL). The mixture was stirred at room temperature for 10 min. Then *N*-hydroxysuccinimide-activated platinum(IV) complex (6.3 mg, 8.7 μmol) in DMSO (0.5 mL) was added quickly to the above mixture. The reaction was continued with stirring at room temperature for another 24 h. The final product was purified by HPLC and lyophilized under vacuum to yield the prodrug as white powders in 40% yield (7.4 mg). ^{1}H NMR (DMSO-d_6, 400 MHz): 12.24 (s, 3H, −COOH), 8.55 (d, 1H, −NH−), 8.51 (d, 1H, −NH−), 8.31 (d, 1H, −NH−), 8.15−8.05 (m, 6H, −NH−), 7.91 (d, 1H, −NH−), 7.86 (s, 1H, −CH−), 7.62 (d, 2H, −NH−), 7.56 (d, 1H, −NH−), 7.45 (m, 1H, −NH−), 7.22−7.06 (m, 6H, −CH−), 7.02−6.99 (m, 5H, −CH−), 6.95−6.88 (m, 4H, −CH−), 6.82−6.79 (m, 4H, −CH−), 6.60−6.35 (m, 6H, $-NH_3$), 5.45 (s, 2H, $-CH_2-$), 4.65−4.60 (m, 1H, −CH−), 4.54−4.48 (m, 1H, −CH−), 4.40−4.32 (m, 3H, −CH−), 4.17−4.10 (m, 3H, −CH−), 4.05−4.02 (m, 1H, −CH−), 3.95−3.91 (m, 1H, −CH−), 3.10−3.06 (m, 4H, $-CH_2-$), 2.95−2.87 (m, 2H, $-CH_2-$), 2.85−2.78 (m, 2H, $-CH_2-$), 2.75−2.62 (m, 6H, $-CH_2-$), 2.50−2.45 (m, 8H, $-CH_2-$), 2.27−2.23 (m, 4H, $-CH_2-$), 1.93−1.89 (m, 4H, $-CH_2-$), 1.72 (m, 2H, $-CH_2-$), 1.41−1.38 (m, 2H, $-CH_2-$), 1.37−1.32 (m, 2H, $-CH_2-$), 0.84−0.74 (m, 6H, $-CH_3$), 0.43 (s, 6H, $-CH_3$); ESI-MS: m/z $[M + H]^+$ calcd 2141.719, found 2141.689.

General Procedure for Enzymatic Assay. DMSO stock solutions of TPS-DEVD-Pt-cRGD were diluted with a mixture of DMSO and PIPES (v/v = 1/199) to 10 μM. Next, each probe was incubated with ascorbic acid or caspase-3 at room temperature, and the change of fluorescence intensity was measured. The PL spectra were collected from 420 to 650 nm under excitation at 365 nm.

Cell Culture. U87-MG human glioblastoma cancer cells, MCF-7 breast cancer cells, and 293T normal cells were provided by American Type Culture Collection (ATCC). The cells were cultured in DMEM (Invitrogen, Carlsbad, CA) containing 10% heat-inactivated FBS (Invitrogen), 100 U/mL penicillin, and 100 μg/mL streptomycin (Thermo Scientific) and were maintained in a humidified incubator at 37 °C with 5% CO_2. Before experiment, the cells were precultured until confluence was reached.

Confocal Imaging. U87-MG, MCF-7, and 293T cells were cultured in the chambers (LAB-TEK, Chambered Coverglass System) at 37 °C. After 80% confluence, the culture medium was removed, and the cells wefre washed twice with PBS buffer. The probe in DMSO stock solution was then added to the chamber to reach a final concentration of 5 μM. In some experiments, the cells were preincubated with media containing cRGD (50 μM) or inhibitor (5 μM) prior to prodrug incubation. After incubation with the prodrug at 37 °C for 2 h, the medium was replaced with fresh medium and further incubated for different times. Then the cells were washed twice with ice-cold PBS, and the cell nuclei were live stained with DRAQ5 (Biostatus) following the standard protocol of the manufacturer. For colocalization with active caspase-3 antibody, the cells were first fixed for 15 min with 3.7% formaldehyde in 1 × PBS at room temperature, washed twice with cold PBS again, and permeabilized with 0.1% Triton X-100 in PBS for 10 min. The cells were then blocked with 2% BSA in 1 × PBS for 30 min and washed twice with PBS. The cells were subsequently incubated with a mixture of anti-caspase-3 antibody/PBS (v/v = 1/99) for 1 h at room temperature, washed once with PBS buffer, and then incubated with mouse anti-rabbit IgG-TR (0.8 μg mL^{-1}) in PBS for 1 h, followed by washing with PBS. The cells were then imaged immediately by confocal laser scanning microscope (CLSM, Zeiss LSM 410, Jena, Germany). The images were analyzed by Image J 1.43 × program (developed by NIH, http://rsbweb.nih.gov/ij/).

Quantification of Cell Apoptosis by Fluorescence Microplate Reader. U87-MG and MCF-7 cells were seeded in 96-well plates (Costar, United States) at an intensity of 4 × 10^4 cells mL^{-1}. After confluence, the medium was replaced by different concentrations of TPS-DEVD-Pt-cRGD in fresh FBS-free DMEM medium for 2 h. After the determined incubation time at 37 °C, the adherent cells were washed twice with 1× PBS buffer followed by fluorescence measurement using a T-CAN microplate reader. The excitation and emission wavelengths are 365 and 480 nm, respectively.

Cytotoxicity of the Prodrug. 3-(4,5-Dimethythiazol-2-yl)-2,5-diphenyltetrazolium bromide (MTT) assays were used to assess the metabolic activity of U87-MG and MCF-7 cancer cells. The cells were seeded in 96-well plates (Costar, IL, United States) at an intensity of 4 × 10^4 cells mL^{-1}. After 24 h incubation, the medium was replaced by the probe suspension at different concentration of the prodrug and incubated at 37 °C for 6 h. After the designated time intervals, the wells were washed twice with 1× PBS buffer, and 100 μL of freshly prepared MTT (0.5 mg mL^{-1}) solution in culture medium was added into each well. The MTT medium solution was carefully removed after 3 h incubation in the incubator at 37 °C. DMSO (100 μL) was then added into each well and the plate was gently shaken to dissolve all the precipitates formed. The absorbance of MTT at 570 nm was monitored by the microplate reader (Genios Tecan). Cell viability was expressed by the ratio of absorbance of the cells incubated with prodrug suspension to that of the cells incubated with culture medium only.

■ RESULTS AND DISCUSSION

Azide-functionalized tetraphenylsilole (TPS-CH_2N_3) was synthesized by the heterobifunctional modification of dimethylbis-(phenylethynyl)silane with 4-bromobenzene and 4-bromobenzyl azide. Detailed synthesis and characterization of TPS-CH_2N_3 and the intermediates are shown in the Experimental Section and Supporting Information (SI) (Scheme S1, Figures S1−S2). The coupling between TPS-CH_2N_3 and alkyne-functionalized DEVD via "click" reaction using $CuSO_4$/sodium ascorbate as the catalyst in DMSO/water (v/v = 1/1) afforded amine terminated TPS-DEVD in 45% yield after HPLC purification (Scheme S2, SI). The purity and identity of the probe was well characterized by analytical HPLC, NMR, and HRMS (Figures S3−S5, SI). Commercially available anticancer drug cisplatin was modified to be used as the linker between amine terminated TPS-DEVD and the amine functionalized cRGD (Scheme S3, SI). In the first step, cisplatin was oxidized by hydrogen peroxide to produce *cis, cis, trans*-diaminedichlorodihydroxyplatinum(IV) complex. Next, the Pt(IV) complex was reacted with succinic anhydride in DMSO at 70 °C for 12 h to yield *cis, cis, trans*-diamminedichlorodisuccinatoplatinum(IV) complex (Figures S6−S7, SI). The activated Pt(IV) complex was subsequently obtained by reacting the carboxylic acid groups with NHS in anhydrous DMF using EDC as the coupling reagent. The activated Pt(IV) linker was purified by HPLC and lyophilized as white powder with 78% yield (Figures S8−S11, SI).

dx.doi.org/10.1021/ja411811w | J. Am. Chem. Soc. 2014, 136, 2546−2554

Scheme 2. Synthetic Route to the Theranostic Prodrug of TPS-DEVD-Pt-cRGD

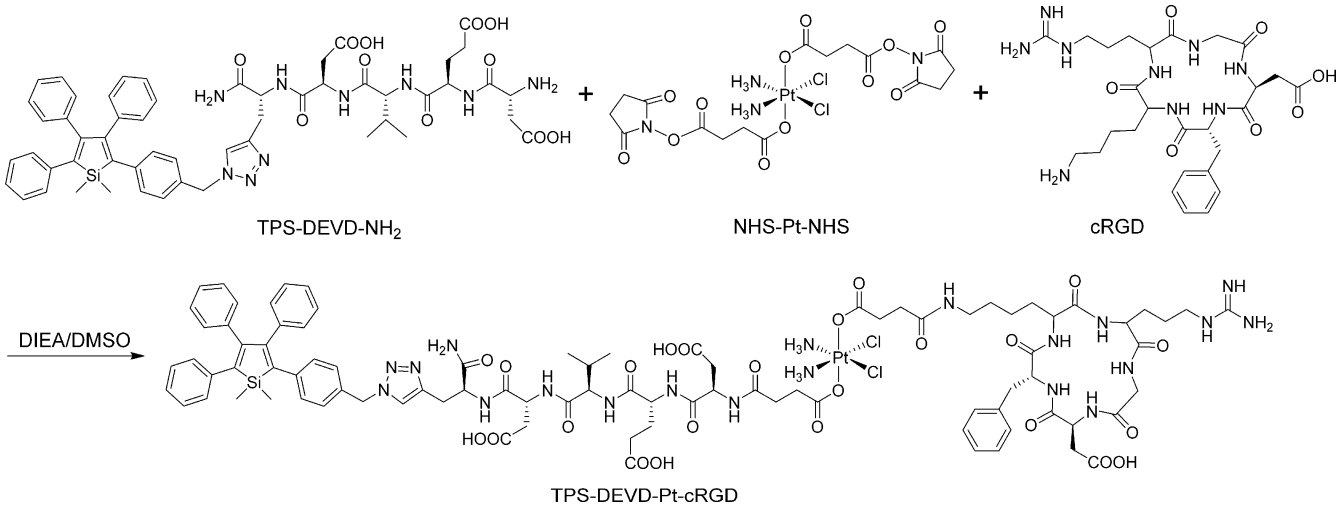

Asymmetric functionalization of activated Pt(IV) linker with amine-terminated TPS-DEVD and amine-functionalized cRGD in the presence of *N*,*N*-diisopropylethylamine (DIEA) in anhydrous DMSO afforded the desired product, TPS-DEVD-Pt-cRGD in 40% yield after HPLC purification (Scheme 2). The purity and identity of the probe was well characterized by HPLC, NMR, and HRMS (Figures S12−S14, SI).

For any prodrug, it is essential that it can be easily transformed into its original form to restore its therapeutic ability after the modification. To evaluate our prodrug as a potential drug delivery system, we studied the nature of the formed Pt(II) species upon reduction of the synthesized prodrug. It is reported that diethyldithiocarbamate (DDTC) is inert to Pt(IV) complexes, but can react with Pt(II) complexes to yield the adduct of $Pt(DDTC)_2$.[15] In this work, we used HPLC−MS to monitor the adduct formation for Pt(IV) complexes before and after treatment with ascorbic acid in the presence of DDTC. We chose ascorbic acid as a reduction agent because its abundance in cells (1 mM), which has been demonstrated to be a major substance for the reduction of Pt(IV).[12c] As shown in Figure 1, cisplatin can efficiently bind to DDTC to form the adduct of $Pt(DDTC)_2$. The complex was further confirmed by IT-TOF with a mass-to-charge ratio (m/z) of 492.104 (Figure S15, SI). On the other hand, $Pt(DDTC)_2$ is only formed when the prodrug is treated with ascorbic acid and in the presence of DDTC, confirming that the released Pt entities are indeed Pt(II) species. In addition, an apoptosis sensor TPS-DEVD with an m/z of 1140.344 is formed after the reduction (Figure S16, SI) and this fraction was collected and lyophilized for further use. Based on these results, we confirm that the Pt(IV) prodrug can be reduced in the presence of ascorbic acid to generate the reactive Pt(II) drug and apoptosis sensor simultaneously.

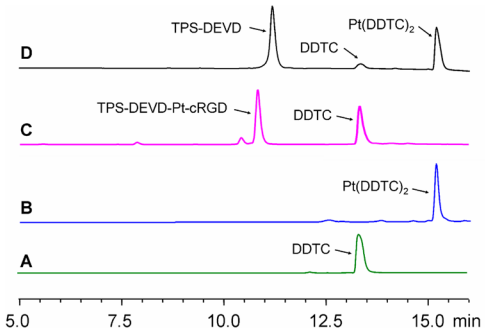

Figure 1. HPLC spectra showing the reaction of diethyldithiocarbamate (DDTC) with cisplatin and reduced Pt(IV) prodrug: (A) DDTC alone; (B) the product for reaction between DDTC and cisplatin; (C) the mixture of DDTC and TPS-DEVD-Pt-cRGD; (D) the products for the reaction between DDTC with TPS-DEVD-Pt-cRGD (10 μM) after treated with 1 mM ascorbic acid for 12 h.

We next studied the optical properties of the prodrug. The UV−vis absorption spectra of TPS-CH_2N_3 in THF and TPS-DEVD-Pt-cRGD in DMSO/PIPES (v/v = 1/199) buffer are shown in Figure S17A, SI. Both have a similar absorption profile in the 320−440 nm range. It is known that AIE fluorogen is nonemissive in good solvents but emits intensely in solid or as aggregates in poor solvents.[9b,c] As can be seen from the photoluminescence (PL) spectra shown in Figure 2A, TPS-CH_2N_3 shows intense fluorescence in DMSO/PIPES (v/v = 1/199), while the TPS-DEVD and TPS-DEVD-Pt-cRGD are almost nonfluorescent in the same medium, due to their good solubility in water. The aggregate formation for hydrophobic TPS-CH_2N_3 in DMSO/PIPES (v/v = 1/199) buffer was confirmed by laser light scattering (LLS) measurement, which shows an average diameter of 118 nm (Figure S17B, SI). As biosensing is often conducted in buffers, it is important to study the effect of ionic strength on the emission behavior of the prodrug. The experiments were performed by adding sodium chloride into an aqueous solution of TPS-DEVD-Pt-cRGD or TPS-DEVD (10 μM). Almost no change in fluorescence intensity is observed for both when the concentration of NaCl is increased from 0 to 960 mM (Figure S18A, SI). Their PL profiles also do not change in the commonly used medium Dulbecco's Modified Eagle Medium (DMEM). Due to the low pK_a value of carboxyl groups in DEVD, the prodrug remains almost nonfluorescent in slightly acidic conditions (pH 5.5, Figure S18B, SI). Based on the above results, we know that TPS-DEVD-Pt-cRGD and the apoptosis sensor TPS-DEVD maintain an "off" state in the complex environment and thus have great potential to serve as a specific light-up apoptosis sensor for drug effect study with minimum background interference.

Figure 2B shows the optical properties of the prodrug before and after reduction with ascorbic acid. There is no fluorescence

dx.doi.org/10.1021/ja411811w | *J. Am. Chem. Soc.* 2014, 136, 2546−2554

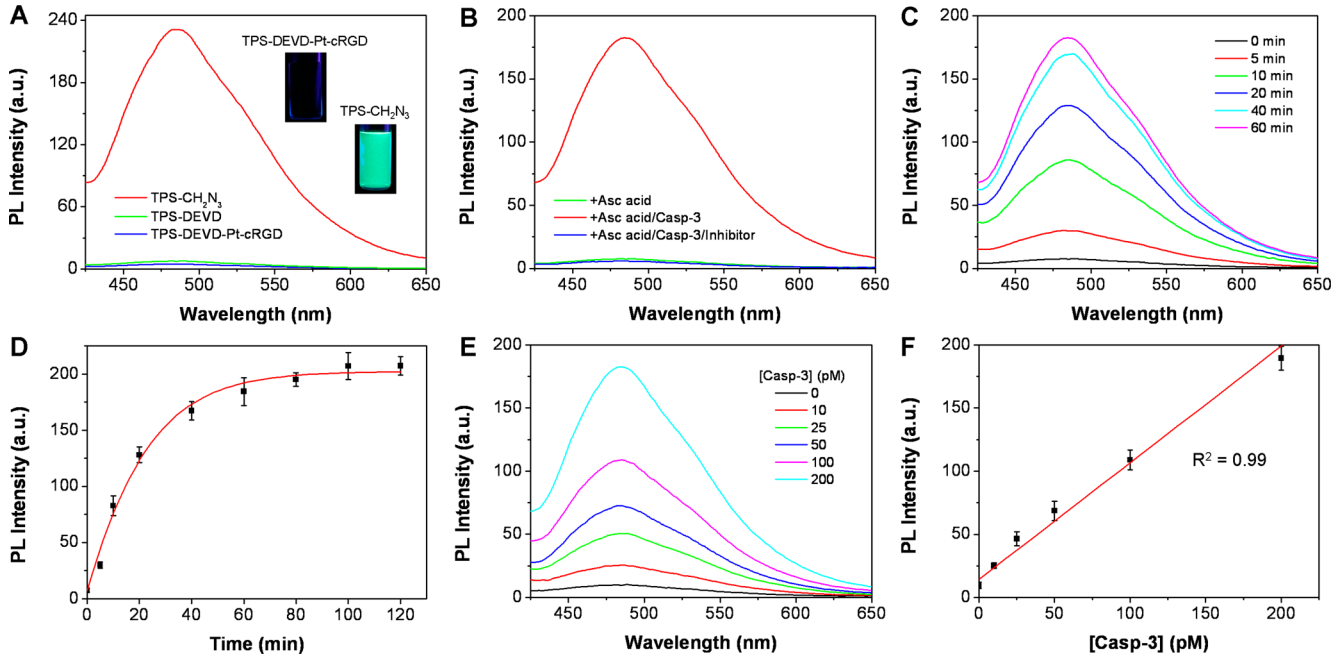

Figure 2. (A) PL spectra of TPS-CH_2N_3, apoptosis sensor TPS-DEVD, TPS-DEVD-Pt-cRGD in DMSO/PIPES (v/v = 1/199). Inset: Corresponding photographs taken under illumination of a UV lamp at 365 nm. (B) PL spectra of TPS-DEVD-Pt-cRGD upon treatment with ascorbic acid and caspase-3 in the presence and absence of inhibitor 5-[(S)-(+)-2-(methoxymethyl)pyrrolidino] sulfonylisatin (10 μM). (C) Time-dependent fluorescence spectra of TPS-DEVD-Pt-cRGD in the presence of caspase-3 in DMSO/PIPES buffer (v/v = 1/199) after the treatment with ascorbic acid. (D) PL intensity at 480 nm of ascorbic acid (1 mM) pretreated TPS-DEVD-Pt-cRGD (10 μM) upon addition of caspase-3 (200 pM) from 0 to 120 min. Data represent mean values ± standard deviation, n = 3. (E) PL spectra of ascorbic acid (1 mM) pretreated TPS-DEVD-Pt-cRGD (10 μM) upon incubation with various amounts of caspase-3 (0, 10, 25, 50, 100, and 200 pM) in DMSO/PIPES buffer (v/v = 1/199) for 60 min. (F) PL intensity at 480 nm for ascorbic acid (1 mM) pretreated TPS-DEVD-Pt-cRGD (10 μM) upon addition of various amounts of caspase-3 in DMSO/PIPES buffer (v/v = 1/199) for 60 min. Data represent mean values ± standard deviation, n = 3.

change when TPS-DEVD-Pt-cRGD is reduced to the apoptosis sensor TPS-DEVD. However, strong fluorescence signals are recorded for ascorbic acid pretreated TPS-DEVD-Pt-cRGD (10 μM) upon further treatment with recombinant human caspase-3 (200 pM). In addition, most of the fluorescence is readily competed away by pretreatment of the prodrug with 5-[(S)-(+)-2-(methoxymethyl)pyrrolidino]sulfonylisatin, a highly specific inhibitor of caspase-3,[16] indicating that specific cleavage of DEVD from the apoptosis sensor TPS-DEVD is inhibited. The caspase-3 catalyzed hydrolysis was further confirmed by LC-MS with the formation of TPS residue with an m/z of 582.659 (Scheme S4, Figures S19–S20, SI). After treatment with caspase-3, the TPS residue forms nanoparticles with an average diameter of 109 nm, which explains the solution fluorescence "turn on" (Figure S21, SI).

The fluorescence change of the TPS-DEVD-Pt-cRGD solution (10 μM) upon addition of ascorbic acid and caspase-3 enzyme was also monitored over time in a mixture of DMSO/PIPES (v/v = 1/199) buffer. As shown in Figure 2C, a quick fluorescence increase in solution is observed after incubation with caspase-3. The fluorescence reaches a plateau in 60 min which is 28-fold higher than the intrinsic emission of the prodrug (Figure 2D). We further studied the effect of caspase-3 concentration on the solution emission. Different concentrations of caspase-3 ranging from 0 to 200 pM were incubated in DMSO/PIPES (v/v = 1/199) buffer with TPS-DEVD-Pt-cRGD (10 μM) for 1 h, and the corresponding spectra are shown in Figure 2E. With increasing concentrations of caspase-3, the PL intensities are gradually enhanced due to the increased amount of TPS aggregates formed in aqueous media. As shown in Figure 2F, the plot of PL intensities at 480 nm against the caspase-3 concentration gives a perfect linear line (R^2 = 0.99), suggesting the possibility of caspase-3 quantification on the basis of the PL intensity changes. The detection limit for caspase-3 was estimated to be 1 pM on the basis of the 3×σ method.

To study the selectivity of the prodrug, we incubated ascorbic acid-pretreated TPS-DEVD-Pt-cRGD (10 μM) with several proteins, including lysozyme, pepsin, bovine serum albumin (BSA), and trypsin under identical conditions. As shown in Figure 3A, only caspase-3 displays a 28-fold fluorescence increase, whereas the intensities from other proteins remain low, confirming that DEVD is specifically recognized and cleaved by caspase-3. In addition, among the enzymes in the caspase family, only caspase-3 and -7 can cleave the DEVD peptide (Figure S22, SI). These results demonstrate that the released TPS-DEVD can be used as a specific indicator of caspase-3/-7 in the cells. As ascorbic acid and many different kinds of proteins and enzymes exist inside the cells, we further obtained the cellular lysate of normal and apoptotic U87-MG cells, which were pretreated with commonly used cell apoptosis-inducer staurosporine (STS, 2 μM) to activate the caspase-3/-7 enzymes in the cells.[17] The cell lysates were directly incubated with TPS-DEVD-Pt-cRGD (5 μM), and the fluorescence intensity at 480 nm was monitored over time. As shown in Figure 3B, the fluorescence intensity increases quickly in a way similar to that of the solution study in Figure 2C. Meanwhile, the fluorescence intensity at 480 nm shows a minimum change after incubation with the normal cell lysate without staurosporine treatment, indicating that the apoptosis sensor is highly stable upon treatment with cellular proteins where caspase is not present.

dx.doi.org/10.1021/ja411811w | J. Am. Chem. Soc. 2014, 136, 2546–2554

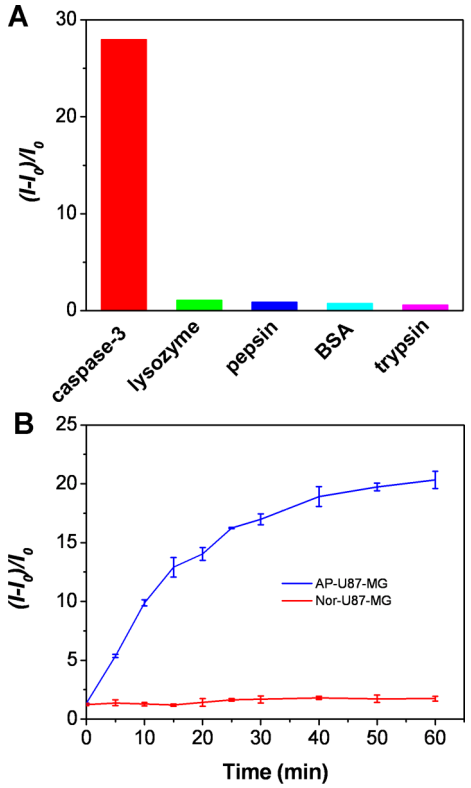

Figure 3. (A) Plot of $(I - I_0)/I_0$ for TPS-DEVD-Pt-cRGD upon incubation with different proteins for 60 min, where I and I_0 are the PL intensities at protein concentrations of 200 and 0 pM, respectively. (B) Time-dependent PL intensity change of TPS-DEVD-Pt-cRGD in apoptotic U87-MG cell lysate (AP-U87-MG) and normal U87-MG cell lysate (Nor-U87-MG). Data represent mean values ± standard deviation, $n = 3$.

To explore the capability of using TPS-DEVD-Pt-cRGD as a targeted drug delivery system and a drug-induced apoptosis imaging sensor in cancer cells, we first incubated TPS-DEVD-pretreated U87-MG cells with cisplatin or STS and monitored their fluorescence changes with confocal microscopy (Figure S23, SI). It can be seen that strong fluorescence signals are collected from the cells treated with cisplatin or STS, as both can activate the caspase activity. These results demonstrate that TPS-DEVD can be used as an indicator of cell apoptosis. To further evaluate whether the probe can be used to quantify the efficiency of apoptosis-inducing agents, TPS-DEVD-pretreated U87-MG cells were treated with different concentrations of cisplatin, and the fluorescence intensity was studied. As shown in Figure S24, SI, with increasing concentration of cisplatin used, the cell fluorescence is progressively intensified, indicating that our probe can be used for semiquantitative analysis of apoptosis-related drug efficacy in living cells. Next, we incubated the prodrug TPS-DEVD-Pt-cRGD with U87-MG human glioblastoma, MCF-7 breast cancer cells and normal 293T cells. The confocal imaging results are shown in Figure 4. U87-MG cells with overexpressed $\alpha_v\beta_3$ integrin on the cellular membrane were chosen as integrin-positive cancer cells, while MCF-7 and 293T cells with low $\alpha_v\beta_3$ integrin expression were used as the negative controls. Upon incubation with TPS-DEVD-Pt-cRGD, the fluorescence of U87-MG cells increases gradually with the cellular apoptotic progress, which reaches a maximum at 6 h. On the contrary, only weak fluorescence signals could be found for MCF-7 and 293T cells within the same period of time. When U87-MG cells were pretreated with free cRGD and/or caspase-3 inhibitor prior to TPS-DEVD-Pt-cRGD incubation, the image shows weak fluorescence (Figure S25, SI). These results clearly demonstrate that TPS-DEVD-Pt-cRGD not only can be used for targeted drug delivery but also has the potential for real-time monitoring of caspase-3 activity in situ. Furthermore, excellent overlap is observed between the confocal images of the TPS residues and immunofluorescence signals generated from anti-caspase-3 primary antibody and a Texas Red-labeled secondary antibody, indicating that the sensor released from the prodrug is specific for cell apoptosis imaging (Figure 5).

Finally, we studied the relationship between the apoptosis-induced fluorescence intensity change and the cytotoxicity profile of the prodrug in U87-MG and MCF-7 cells. After the cells were incubated with different concentrations of TPS-DEVD-Pt-cRGD for 6 h, the fluorescence intensities at 480 nm were monitored upon excitation at 365 nm. As shown in Figure 6A, for U87-MG cells, the fluorescence increases upon incubation with the prodrug in the concentration from 0 to 5 μM, which is followed by saturation. At each prodrug concentration, the cytotoxicity of the corresponding cells was

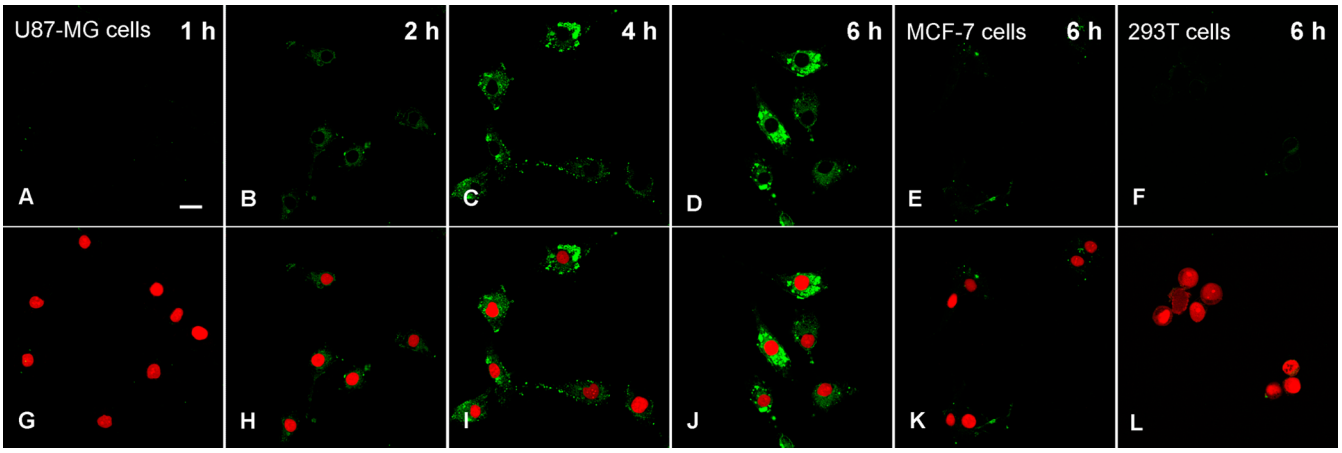

Figure 4. (A–D) Real-time CLSM images displaying the apoptotic progress of TPS-DEVD-Pt-cRGD (5 μM) stained U87-MG cells and confocal images of MCF-7 (E) and 293T (F) cells upon treatment with TPS-DEVD-Pt-cRGD (5 μM) for 6 h. Nuclei were live stained with DRAQ5. (G–L) Corresponding fluorescence/nucleus overlay images of (A–F), respectively. All images share the same scale bar (20 μm).

dx.doi.org/10.1021/ja411811w | J. Am. Chem. Soc. 2014, 136, 2546–2554

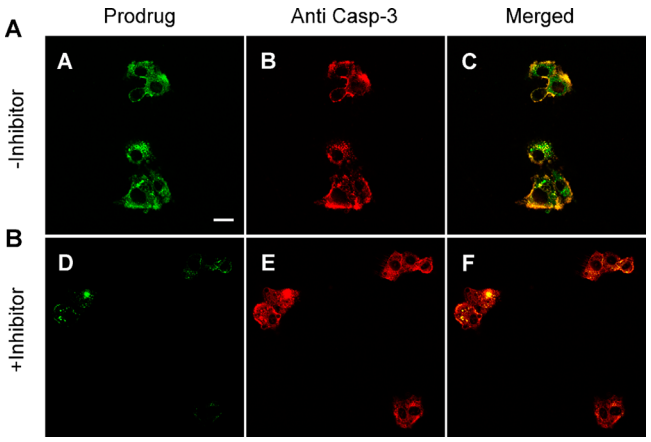

Figure 5. CLSM images of U87-MG cells upon treatment with TPS-DEVD-Pt-cRGD (5 μM) and caspase-3 antibody (A–C) or TPS-DEVD-Pt-cRGD (5 μM) in the presence of inhibitor 5-[(*S*)-(+)-2-(methoxymethyl)pyrrolidino]sulfonylisatin (5 μM) and caspase-3 antibody (D–F). Green = probe fluorescence; red = immunofluorescence signal generated from anti-caspase-3 primary antibody and a Texas Red-labeled secondary antibody. All images share the same scale bar (20 μm).

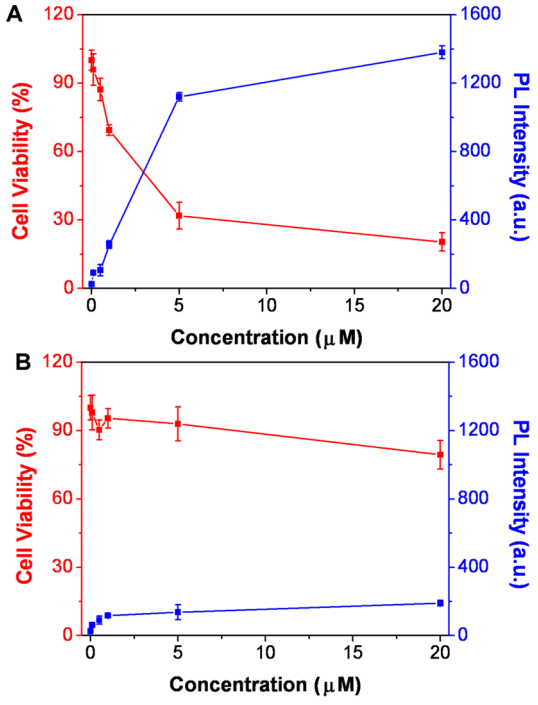

Figure 6. Correlations between cell viability (72 h) determined by MTT assay and apoptosis-induced fluorescence intensity (6 h) of U87-MG (A) and MCF-7 (B) cells upon treatment with TPS-DEVD-Pt-cRGD at different concentrations.

evaluated using a standard MTT assay after overall incubation for 72 h. As the apoptosis sensor TPS-DEVD itself shows no obvious cytotoxicity to the cells (Figure S26, SI), the cell viability change is simply due to the presence of reduced Pt(II) in the cells. As shown in Figure 6A, it is obvious that the cell viability is high when the used prodrug concentration is low and that the cell viability decreases at higher prodrug concentrations. When the same experiments were conducted on MCF-7 cells, the trend is not obvious. These results clearly demonstrate the selective killing effect of the prodrug on U87-MG cells vs MCF-7 cells, which indicates that the prodrug can serve as a targeted drug delivery vehicle and for noninvasive early imaging and semiquantification of its therapeutic response in situ.

CONCLUSIONS

In summary, we report the synthesis and biological application of a theranostic Pt(IV) prodrug for targeted drug delivery and early evaluation of its therapeutic response in situ. The prodrug can be reduced to active Pt(II) inside the cells and simultaneously release the cell apoptosis sensor on its axial position. The reduced Pt(II) can induce the apoptosis of the cancer cell and activate the caspase-3. The activated caspase-3 further cleaves the DEVD sequence of the apoptosis sensor and triggers the AIE effect of TPS residue, thus enabling early evaluation of its therapeutic response in cells with high signal-to-noise ratios. In addition, the apoptosis-induced fluorescence intensity in the U87-MG cells shows a good correlation with the prodrug concentration and the cell viability. These results indicate that the theranostic drug delivery system with a built-in apoptosis sensor allows one to target the drug delivery and evaluate the drug therapeutic response quickly, which is essential to guide therapeutic decisions such as whether the treatment works well or the therapeutic regimes should stop.

ASSOCIATED CONTENT

Supporting Information

Structural characterization data of TPS-CH_2N_3 and TPS-DEVD-Pt-cRGD; absorption spectra of TPS-CH_2N_3 and TPS-DEVD-Pt-cRGD; particle size distribution; in vitro cytotoxicity of TPS-DEVD. This material is available free of charge via the Internet at http://pubs.acs.org.

AUTHOR INFORMATION

Corresponding Authors

cheliub@nus.edu.sg
tangbenz@ust.hk

Notes

The authors declare no competing financial interest.

ACKNOWLEDGMENTS

We thank the Singapore National Research Foundation (R-279-000-390-281), the Ministry of Defense (R279-000-340-232), Singapore-MIT Alliance of Research and Technology (SMART), JCO (IMRE/12-8P1103), and the Research Grants Council of Hong Kong (HKUST2/CRF/10 and N_HKUST620/11) for financial support.

REFERENCES

(1) (a) Langer, R. *Nature* **1998**, *392*, 5–10. (b) Davis, M. E.; Chen, Z.; Shin, D. M. *Nat. Rev. Drug Discov.* **2008**, *7*, 771–782.
(2) Lammers, T.; Aime, S.; Hennink, W. E.; Storm, G.; Kiessling, F. *Acc. Chem. Res.* **2011**, *44*, 1029–1038.
(3) (a) Santra, S.; Kaittanis, C.; Santiesteban, O. J.; Perez, J. M. *J. Am. Chem. Soc.* **2011**, *133*, 16680–16688. (b) Maiti, S.; Park, N.; Han, J. H.; Jeon, H. M.; Lee, J. H.; Bhuniya, S.; Kang, C.; Kim, J. S. *J. Am. Chem. Soc.* **2013**, *135*, 4567–4572. (c) Weinstain, R.; Segal, E.; Satchi-Fainaro, R.; Shabat, D. *Chem. Commun.* **2010**, *46*, 553–555. (d) Zou, T. T.; Lum, C. T.; Chui, S. S. Y.; Che, C. M. *Angew. Chem., Int. Ed.* **2013**, *52*, 2930–2933. (e) Jana, A.; Devi, K. S. P.; Maiti, T. K.; Singh, N. D. P. *J. Am. Chem. Soc.* **2012**, *134*, 7656–7659.
(4) Kuhl, C. K. *Radiology* **2007**, *244*, 672–691.
(5) Hickman, J. A. *Cancer Metastasis Rev.* **1992**, *11*, 121–139.

(6) Schoenberger, J.; Bauer, J.; Moosbauer, J.; Eilles, C.; Grimm, D. *Curr. Med. Chem.* **2008**, *15*, 187−194.
(7) (a) Huang, X.; Swierczewska, M.; Choi, K. Y.; Zhu, L.; Bhirde, A.; Park, J.; Kim, K.; Xie, J.; Niu, G.; Lee, K. C.; Lee, S.; Chen, X. *Angew. Chem., Int. Ed.* **2012**, *51*, 1625−1630. (b) Hu, M.; Li, L.; Wu, H.; Su, Y.; Yang, P. Y.; Uttamchandani, M.; Xu, Q. H.; Yao, S. Q. *J. Am. Chem. Soc.* **2011**, *133*, 12009−12020. (c) Boeneman, K.; Mei, B. C.; Dennis, A. M.; Bao, G.; Deschamps, J. R.; Mattoussi, H.; Medintz, I. L. *J. Am. Chem. Soc.* **2009**, *131*, 3828−3829. (d) Lovell, J. F.; Chan, M. W.; Qi, Q.; Chen, J.; Zheng, G. *J. Am. Chem. Soc.* **2011**, *133*, 18580−18582. (e) Lin, S. Y.; Chen, N. T.; Sun, S. P.; Chang, J. C.; Wang, Y. C.; Yang, C. S.; Lo, L. W. *J. Am. Chem. Soc.* **2010**, *132*, 8309−8315. (f) Barnett, E. M.; Zhang, X.; Maxwell, D.; Chang, Q.; Piwnica-Worms, D. *Proc. Natl. Acad. Sci. U.S.A.* **2009**, *106*, 9391−9396. (g) Dai, N.; Guo, J.; Teo, Y. N.; Kool, E. T. *Angew. Chem., Int. Ed.* **2011**, *50*, 5105−5109. (h) Shen, B.; Jeon, J.; Palner, M.; Ye, D.; Shuhendler, A.; Chin, F. T.; Rao, J. *Angew. Chem., Int. Ed.* **2013**, *52*, 10511−10514.
(8) (a) Shi, H. B.; Kwok, R. T. K.; Liu, J. Z.; Xing, B. G.; Tang, B. Z.; Liu, B. *J. Am. Chem. Soc.* **2012**, *134*, 17972−17981. (b) Shi, H. B.; Zhao, N.; Ding, D.; Liang, J.; Tang, B. Z.; Liu, B. *Org. Biomol. Chem.* **2013**, *11*, 7289−7296.
(9) (a) Hong, Y. N.; Lam, J. W. Y.; Tang, B. Z. *Chem. Commun.* **2009**, 4332−4353. (b) Hong, Y. N.; Lam, J. W. Y.; Tang, B. Z. *Chem. Soc. Rev.* **2011**, *40*, 5361−5388. (c) Ding, D.; Li, K.; Liu, B.; Tang, B. Z. *Acc. Chem. Res.* **2013**, *46*, 2441−2453.
(10) (a) Wang, D.; Lippard, S. J. *Nat. Rev. Drug Discovery* **2005**, *4*, 307−320. (b) Kelland, L. *Nat. Rev. Cancer* **2007**, *7*, 573−584.
(11) Seki, K.; Yoshikawa, H.; Shiiki, K.; Hamada, Y.; Akamatsu, N.; Tasaka, K. *Cancer Chemother. Pharmacol.* **2000**, *45*, 199−206.
(12) (a) Butler, J. S.; Sadler, P. J. *Curr. Opin. Chem. Biol.* **2013**, *17*, 175−188. (b) Dhar, S.; Liu, Z.; Thomale, J.; Dai, H. J.; Lippard, S. J. *J. Am. Chem. Soc.* **2008**, *130*, 11467−11476. (c) Graf, N.; Lippard, S. J. *Adv. Drug Delivery Rev.* **2012**, *64*, 993−1004. (d) Wang, X. Y.; Guo, Z. J. *Chem. Soc. Rev.* **2013**, *42*, 202−224.
(13) Barnes, K. R.; Kutikov, A.; Lippard, S. J. *Chem. Biol.* **2004**, *11*, 557−564.
(14) Liu, J. Z.; Zheng, R. H.; Tang, Y. H.; Haussler, M.; Lam, J. W. Y.; Qin, A.; Ye, M. X.; Hong, Y. N.; Gao, P.; Tang, B. Z. *Macromolecules* **2007**, *40*, 7473−7486.
(15) (a) Lopez-Flores, A.; Jurado, R.; Garcia-Lopez, P. *J. Pharmacol. Toxicol. Methods* **2005**, *52*, 366−372. (b) Li, J.; Yap, S. Q.; Chin, C. F.; Tian, Q.; Yoong, S. L.; Pastorin, G.; Ang, W. H. *Chem. Sci.* **2012**, *3*, 2083−2087.
(16) Lee, D.; Long, S. A.; Adams, J. L.; Chan, G.; Vaidya, K. S.; Francis, T. A.; Kikly, K.; Winkler, J. D.; Sung, C. M.; Debouck, C.; Richardson, S.; Levy, M. A.; DeWolf, W. E.; Keller, P. M.; Tomaszek, T.; Head, M. S.; Ryan, M. D.; Haltiwanger, R. C.; Liang, P. H.; Janson, C. A.; McDevitt, P. J.; Johanson, K.; Concha, N. O.; Chan, W.; Abdel-Meguid, S. S.; Badger, A. M.; Lark, M. W.; Nadeau, D. P.; Suva, L. J.; Gowen, M.; Nuttall, M. E. *J. Biol. Chem.* **2000**, *275*, 16007−16014.
(17) Luhrmann, A.; Nogueira, C. V.; Carey, K. L.; Roy, C. R. *Proc. Natl. Acad. Sci. U.S.A.* **2010**, *107*, 18997−19001.